Seismic Performance of Stainless Steel-Reinforced Concrete Piers: Experimental & Numerical

Xiao Ge, Dong-Sheng Wang
葛　笑　王东升
Hebei University of Technology
河北工业大学

The 7th International Symposium on Ocean Science and

Outline

1. Background
2. Quasi-static tests of SS-reinforced piers
3. Numerical Modelling of SS-reinforced piers
4. Plastic hinge model of SS-reinforced piers
5. Conclusion remarks

Outline

1. Background
2. Quasi-static tests of SS-reinforced piers
3. Numerical Modelling of SS-reinforced piers
4. Plastic hinge model of SS-reinforced piers
5. Conclusion remarks

1 Background

- ***The Cost of Corrosion in China*** was released in 2017
- The corrosion cost for highway bridges reached **¥62.47 billion** in 2014

- **Maintenance costs for existing bridges** could reach up to **$125 billion**
- An **annual budget** of **$22.7 billion** is required to improve structurally deficient bridges

Stonecutters Bridge (2009)

Hong Kong-Zhuhai-Macao Bridge

Champlain Bridge (2019)

➢ In recent years, **stainless steel reinforcement bars** have been widely adopted in coastal and cross-sea bridges to solve **durability issues**.

1 Background

SS Reinforcement Bars:

✓ Corrosion resistance ✓ High strength ✓ Durability ✓ Low maintenance
✓ High-temperature resistance ✓ Fatigue resistance

SS rebar

SS-reinforced concrete piers

SS-Reinforced Concrete Bridges:

✓ Exceptional corrosion resistance ✓ Long service life ✓ Low maintenance costs ✓ High strength and toughness ✓ Eco-friendly sustainability ✓ Special environmental adaptability

1 Background

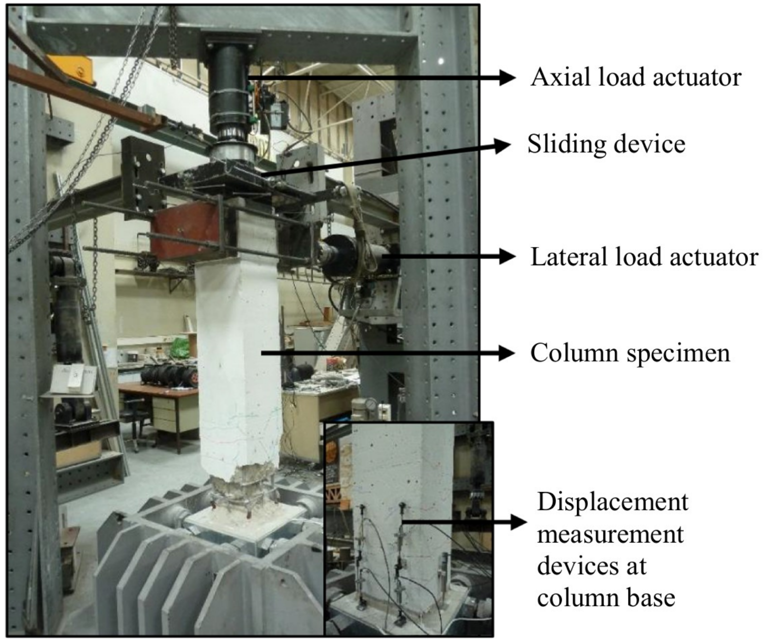

Melo et al. (2022)

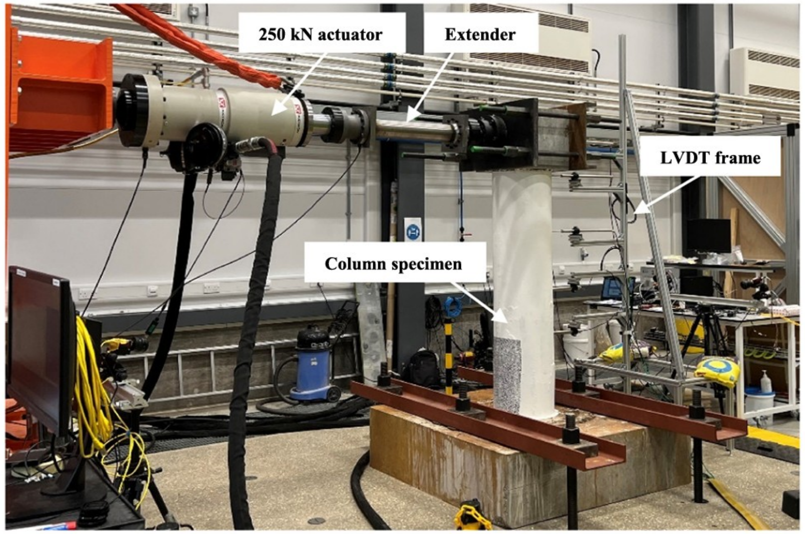

Moodley et al. (2024)

- 3 specimens with height of **1.65m**
- 1.4462 **duplex** stainless steel rebars
- **Pushover** and **quasi-static** tests
- Higher **ultimate strength**
- Better **deformation capacity**

- 3 specimens with height of **2.00m**
- **Duplex** & **austenitic** stainless rebars
- Larger **yield displacement**
- Higher **ultimate strength**
- Better **deformation capacity**

- Melo J, Afshan S, Rossetto T, Varum H, Arêde A. Experimental and numerical investigation of the cyclic response of stainless steel reinforced concrete columns. Engineering Structures. 2022, 252:113607.
- Moodley H, Afshan S, Crump D, Kashani MM. Testing and numerical modelling of circular stainless steel reinforced concrete columns. Engineering Structures. 2024,

1 Background

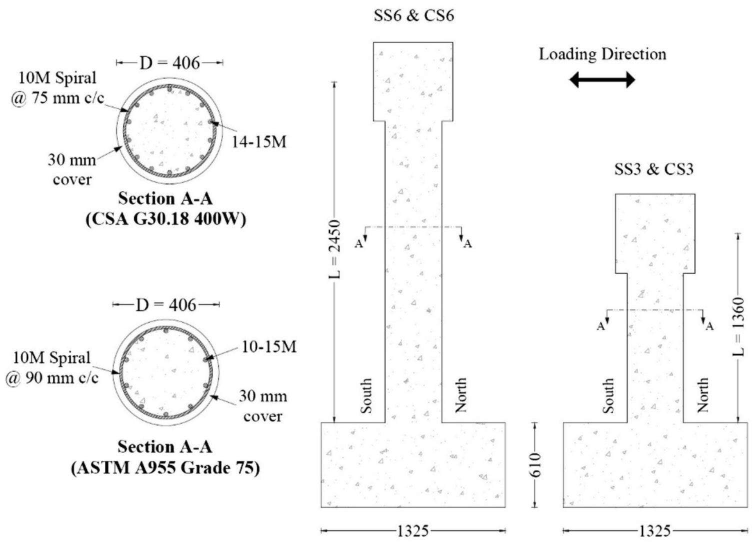

Rodríguez et al. (2025)

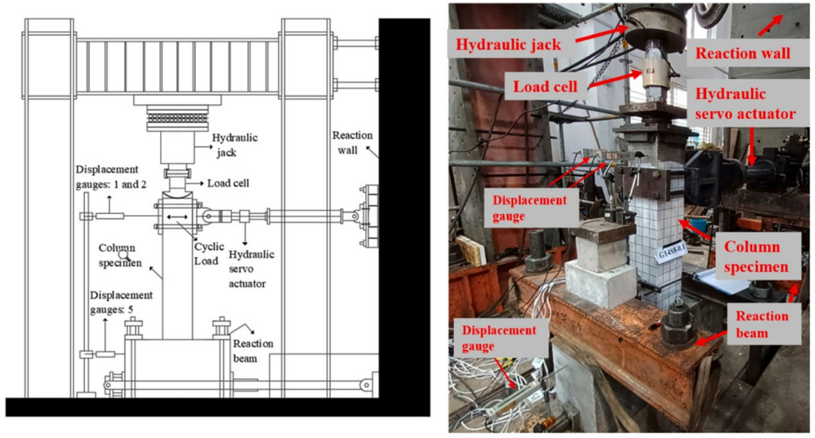

(a) schematic drawing (b) photo view

Cao et al. (2025)

- 4 specimens with height of **2.45m**
- ASTM A955 Grade 75 **SS rebars**
- **Slender ratio** of 3 & 6
- Higher **ultimate strength**
- **Buckling** of SS

- **Hybrid reinforcement** of SS and GFRP
- **Axial ratio** & **hybrid reinforcement ratio**
- Better **deformation capacity**
- Increasing **energy dissipation capacity**

- Rodríguez J, Aldabagh S, Alam MS. Seismic Performance of Circular Concrete Bridge Columns Reinforced with ASTM A955 Stainless Steel Rebars. Journal of Structural Engineering. 2025, 151(4):04025013.
- Cao Q, Ju H, Wu Z, Ma ZJ. Experimental study on seismic performance of GFRP and highly ductile stainless steel hybrid reinforced concrete columns. Engineering Structures. 2025, 322:119130.

1 Background

- Research on the SSRC piers **remains limited** at present.
- Current **codes and standards lack specific provisions** for the seismic design.
- Significant research potential persists across **material properties**, **component behaviour**, and **structural system** performance of SSRC piers.


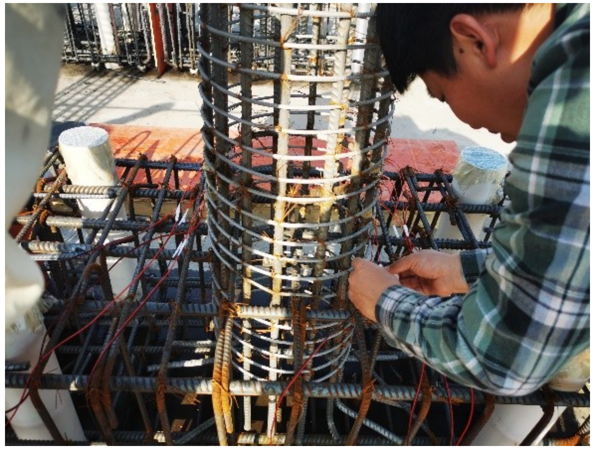



Outline

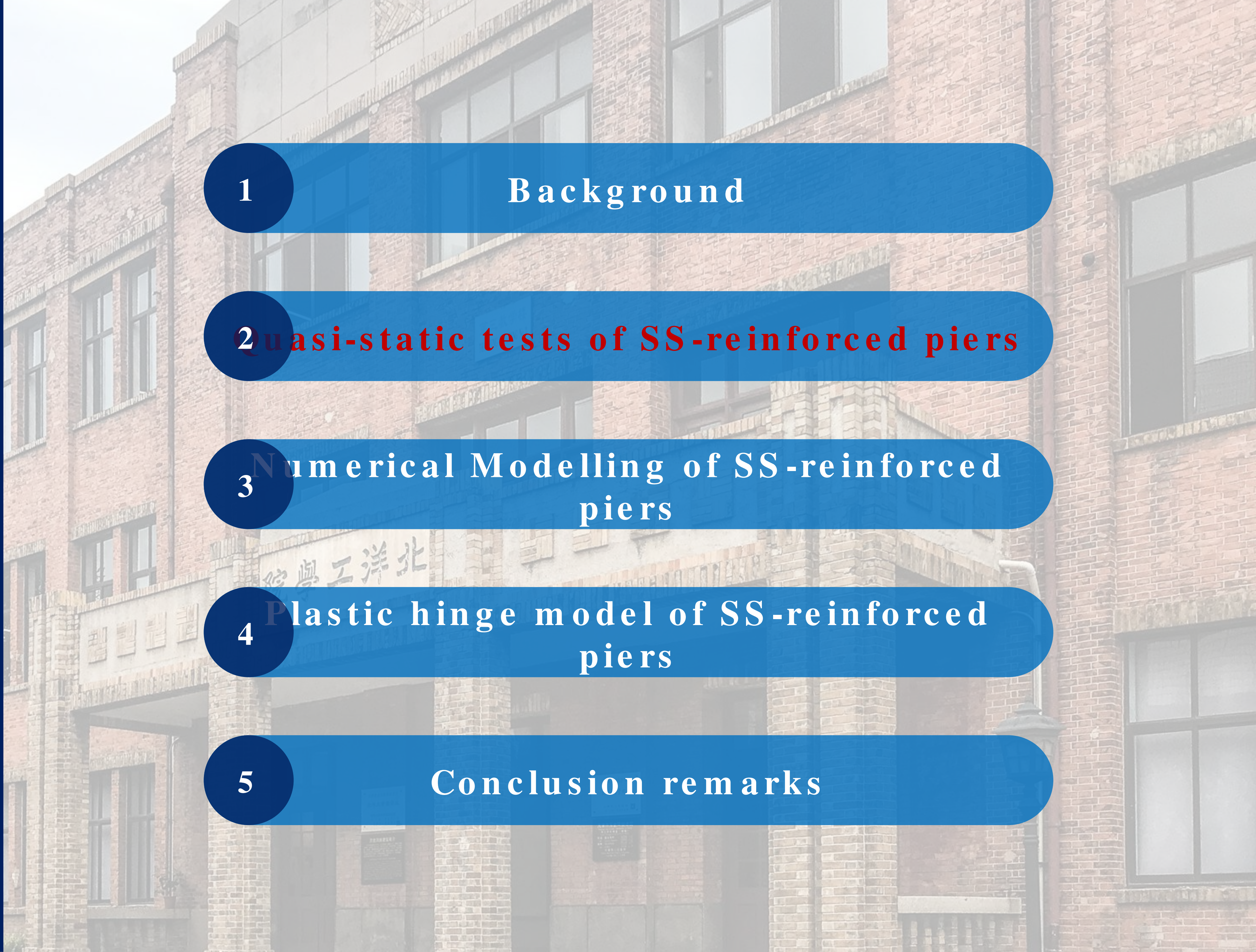

1. Background
2. Quasi-static tests of SS-reinforced piers
3. Numerical Modelling of SS-reinforced piers
4. Plastic hinge model of SS-reinforced piers
5. Conclusion remarks

2 Quasi-static tests of SS-reinforced piers

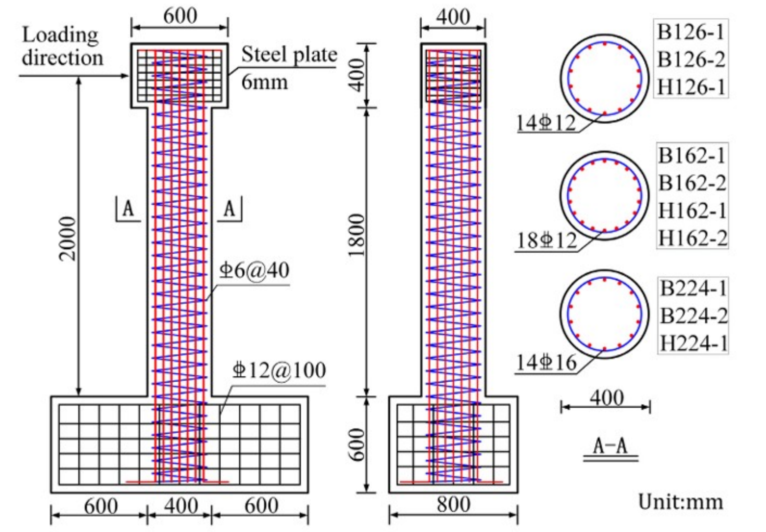

Specimen design

- 10 specimens
- 2m tall
- C55 concrete

DIC

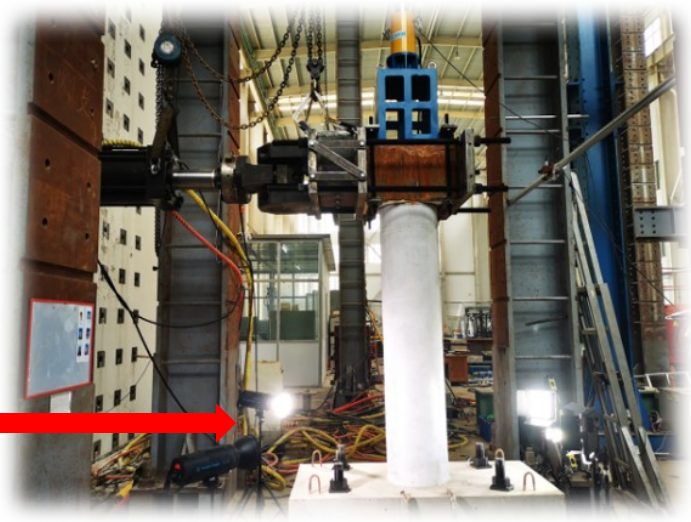

Test setup

Specimen design parameters

Reinforcement ratio | Rebar type | Axial load

Specimen	Vertical bar			Spiral			η
	Diameter	ρ (%)	Type	Diameter	ρ (%)	Type	
B126-01	14D12	1.26	B1.4362	C6@40mm	1.0	B1.4362	0.1
B126-02	14D12	1.26	B1.4362	C6@40mm	1.0	B1.4362	0.2
B162-01	18D12	1.62	B1.4362	C6@40mm	1.0	B1.4362	0.1
B162-02	18D12	1.62	B1.4362	C6@40mm	1.0	B1.4362	0.2
B224-01	14D16	2.24	B1.4362	C6@40mm	1.0	B1.4362	0.1
B224-02	14D16	2.24	B1.4362	C6@40mm	1.0	B1.4362	0.2
H126-01	14D12	1.26	HRB500	C6@40mm	1.0	HRB400	0.1
H162-02	18D12	1.62	HRB500	C6@40mm	1.0	HRB400	0.2
H162-01	18D12	1.62	HRB500	C6@40mm	1.0	HRB400	0.1
H224-02	14D16	2.24	HRB500	C6@40mm	1.0	HRB400	0.2

Quasi-static tests of SS-reinforced piers

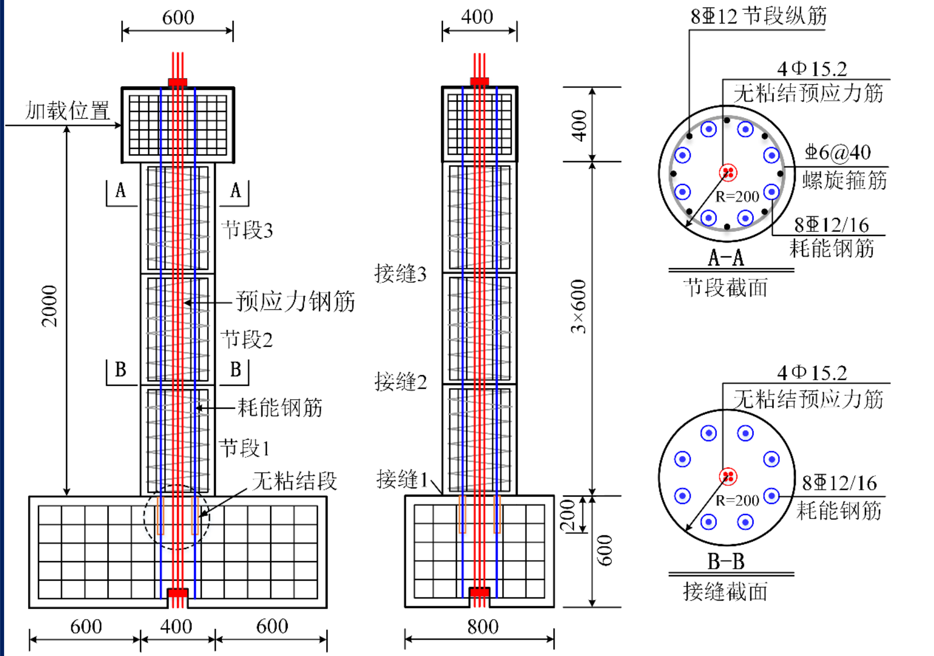

Circular cross-sectional specimens

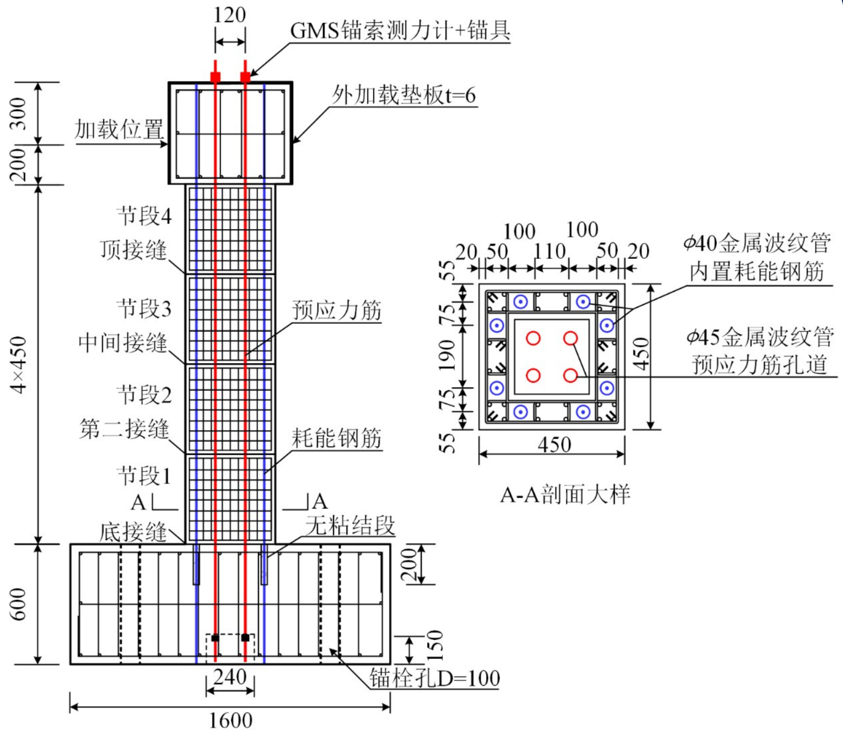

Rectangular hollow cross-sectional specimens

Completed quasi-static tests on **prestressed segmental piers** with **SS energy-dissipating bars** (total: 15 specimens)

- 7 **circular** cross-section prefabricated bridge piers
- 8 **rectangular hollow** cross-section prefabricated bridge piers

Quasi-static tests of SS-reinforced piers

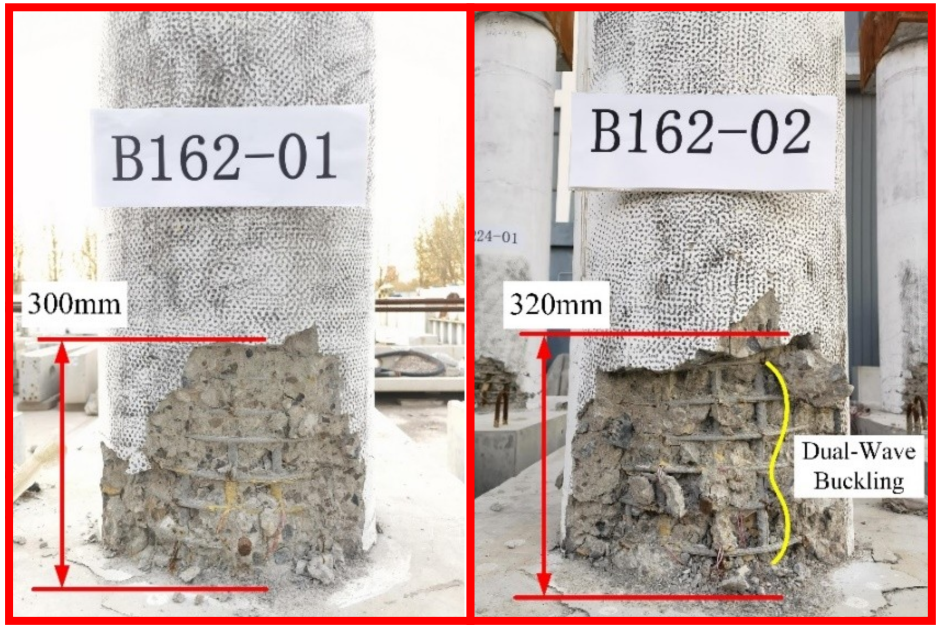

SS-reinforced pier
Reinforcement ratio: 1.62%,
axial load: 0.2

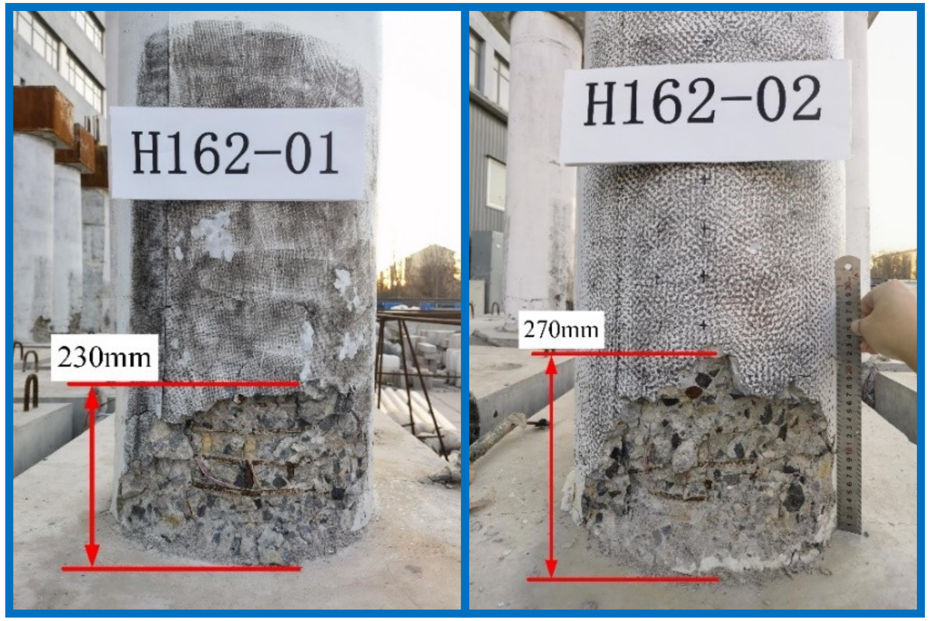

CS-reinforced pier
Reinforcement ratio: 1.62%,
axial load: 0.2

- With **the increase of axial compression ratio**, **the spalling height of concrete cover increases by approximately 5%-20%**.
- The spalling height of concrete cover in SS-reinforced concrete piers is **20%-30% higher** than that in conventional piers.
- B162-02 exhibited **double-wave buckling** of longitudinal reinforcement during the test, which may be attributed to **the low bond strength** between stainless steel rebars and concrete.

2 Quasi-static tests of SS-reinforced piers

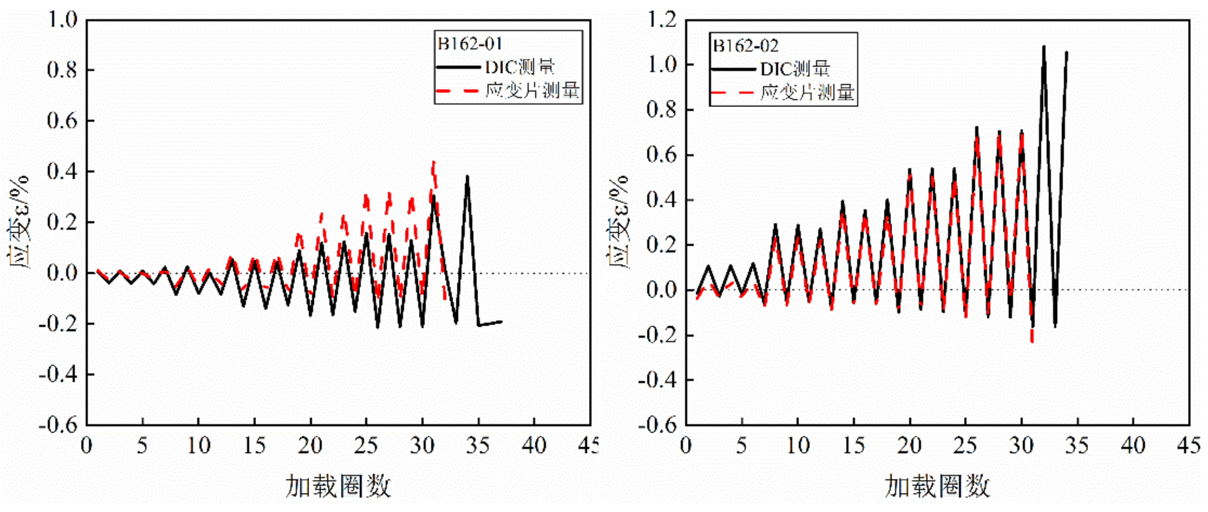

DIC vs strain gauge

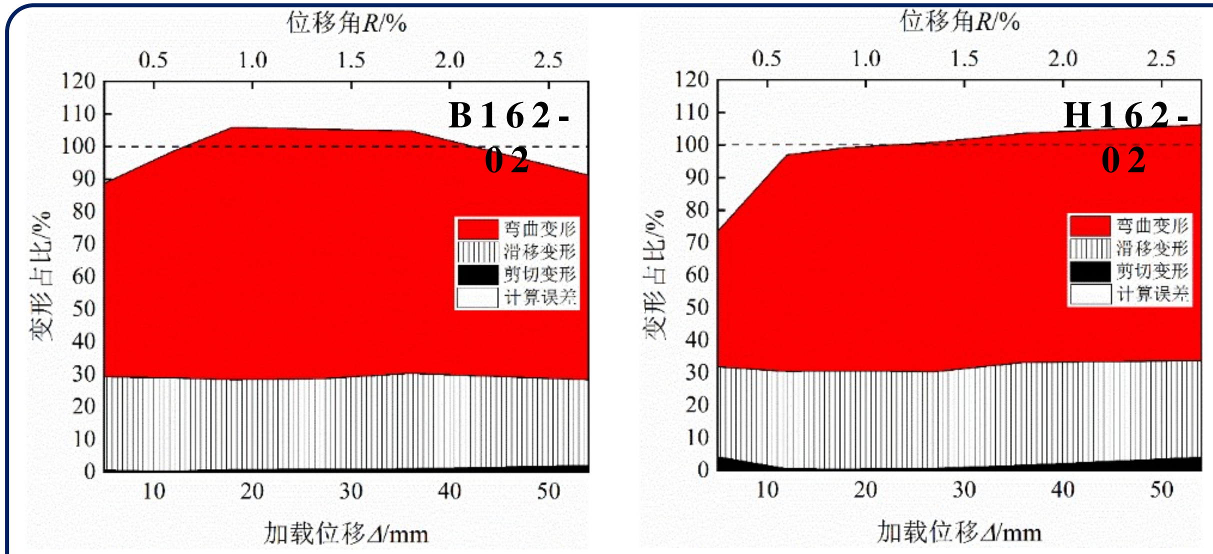

Deformation components

- Deformation components were calculated from **DIC-recorded data**.
- **Flexural deformation component** is 30%~50% in the early loading stage and increases to 70% in the later stage.
- **Slip deformation component** remained stable at 30%~40% throughout the loading process.
- Higher axial ratios **reduce** slip deformation.
- **Shear deformation** consistently accounted for less than 5% in all cases.

2 Quasi-static tests of SS-reinforced piers

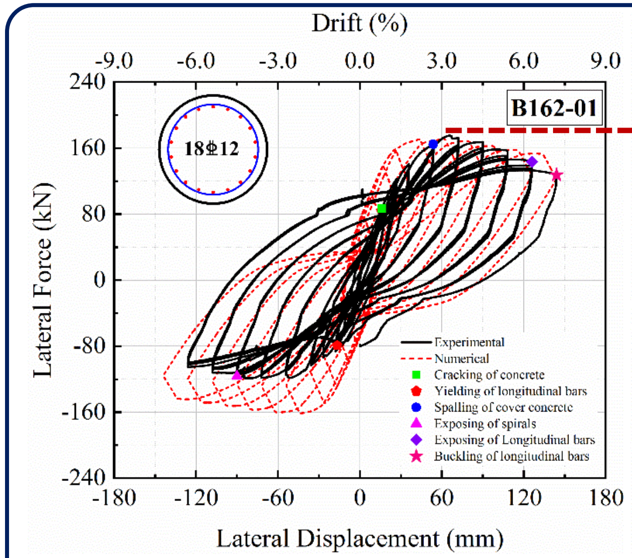

SS specimen

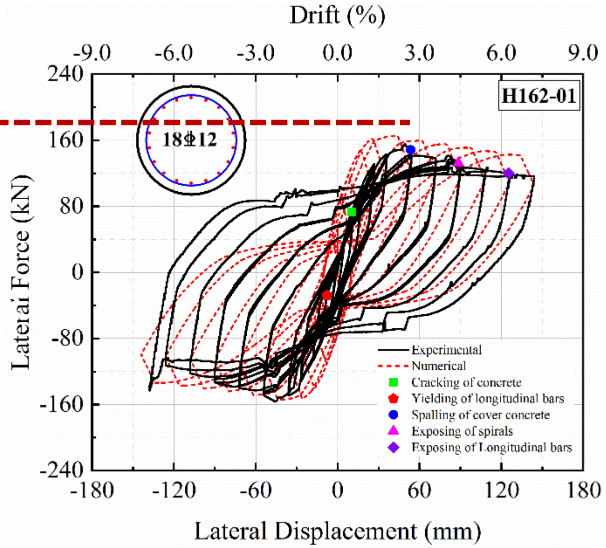

CS specimen

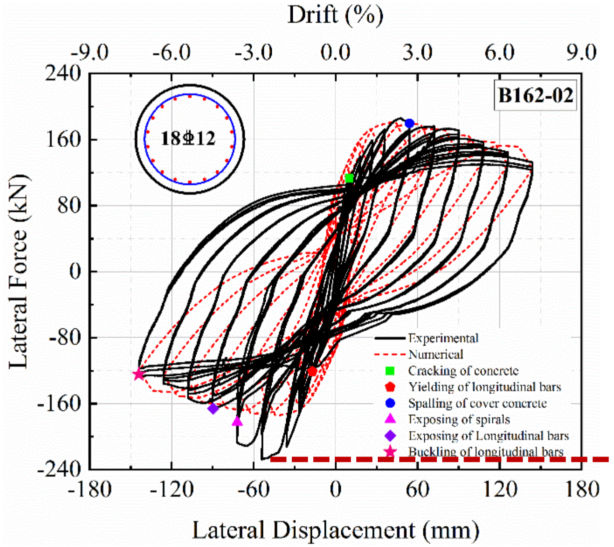

SS specimen

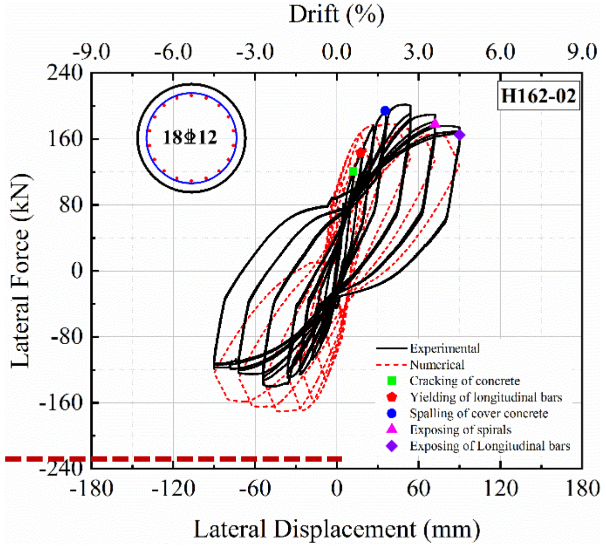

CS specimen

Under the same reinforcement arrangement:

- ➢ **CS piers exhibit fuller hysteresis curves**
- ➢ **SS piers show larger ultimate strength**

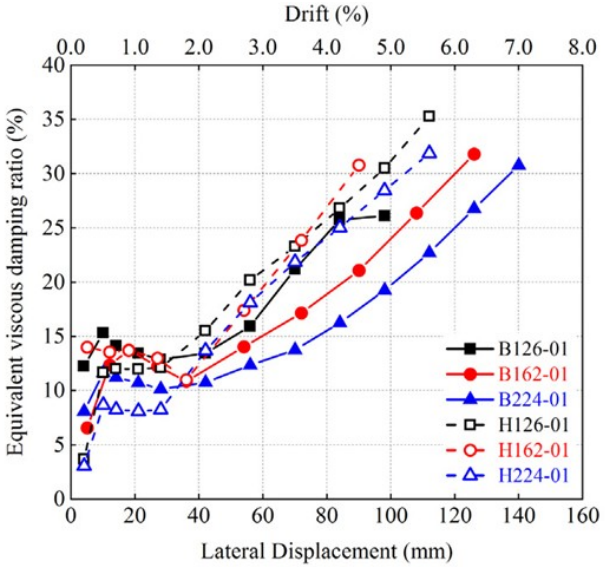

Damping ratio

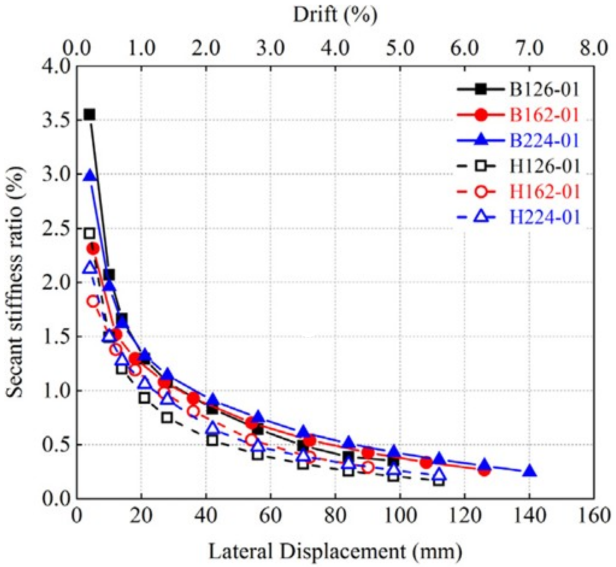

Stiffness ratio

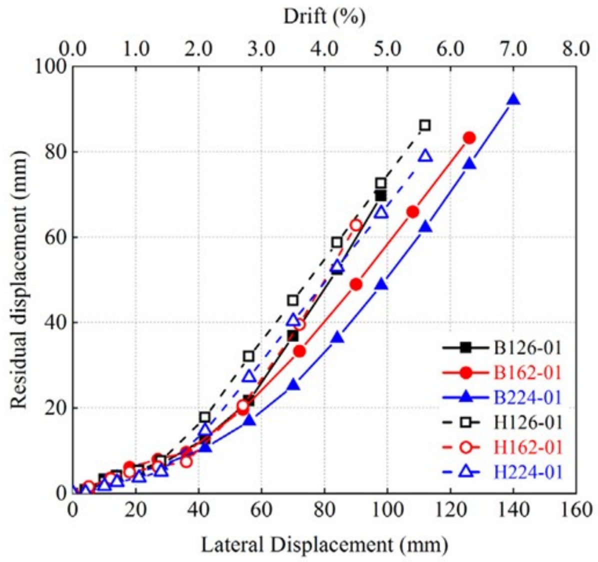

Residual displacement

For piers with identical design parameters:

- SS-reinforced piers exhibit **larger deformation capacity** compared to conventional piers, with maximum drift ratios exceeding 5% in all cases
- The **damping ratio** of SS-reinforced piers is **slightly lower** than that of conventional piers. However, SS specimen demonstrates **greater energy dissipation potential**
- SS-reinforced piers show **higher initial stiffness** than conventional counterparts
- **Stiffness degradation** occurs at a slower rate in SS-reinforced piers
- **Residual displacements** are consistently smaller in SS-reinforced piers

Outline

1. Background
2. Quasi-static tests of SS-reinforced piers
3. Numerical Modelling of SS-reinforced piers
4. Plastic hinge model of SS-reinforced piers
5. Conclusion remarks

3 Numerical Modelling of SS-reinforced piers

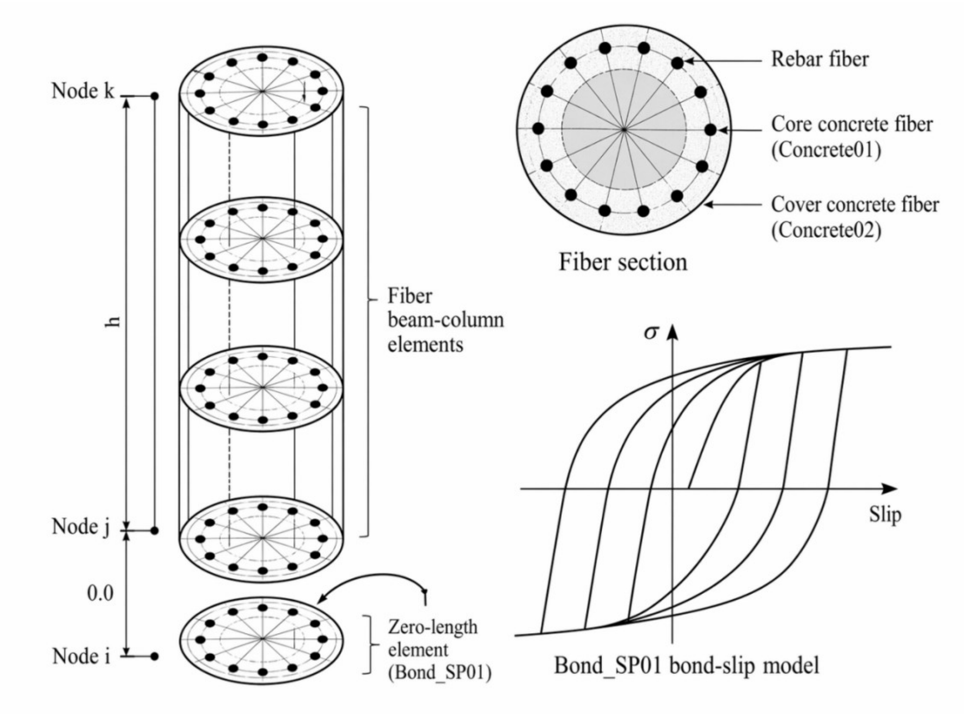

Numerical model established by OpenSees

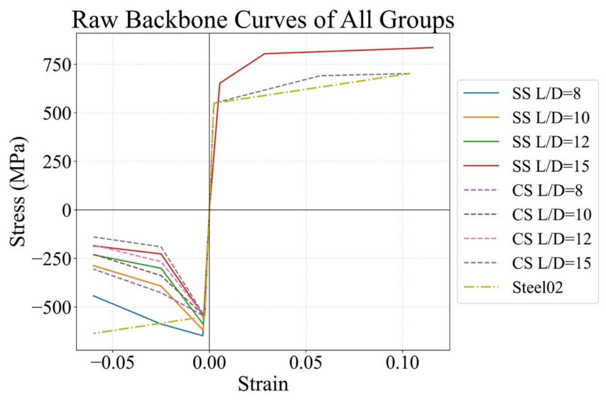

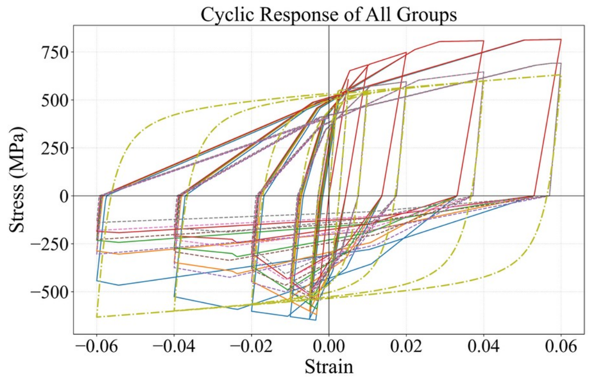

Inelastic buckling

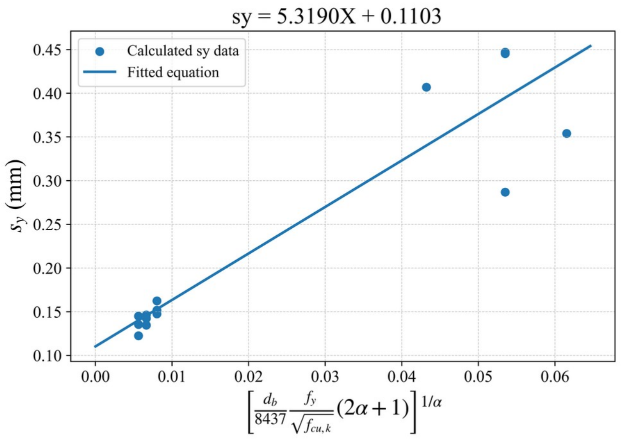

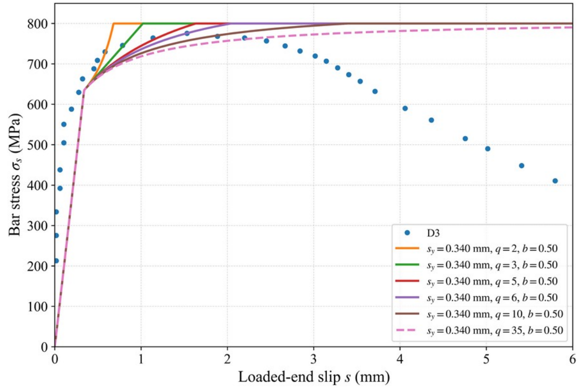

Bond slip effects

Numerical Modelling of SS-reinforced piers

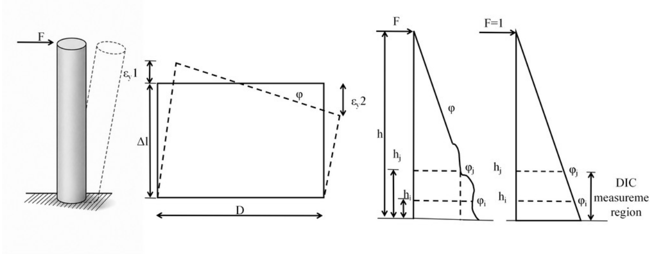

Flexural displacement

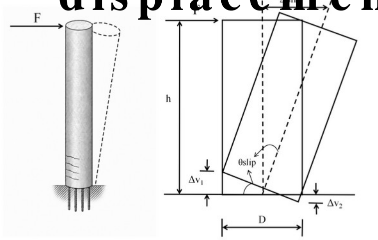

Slip displacement

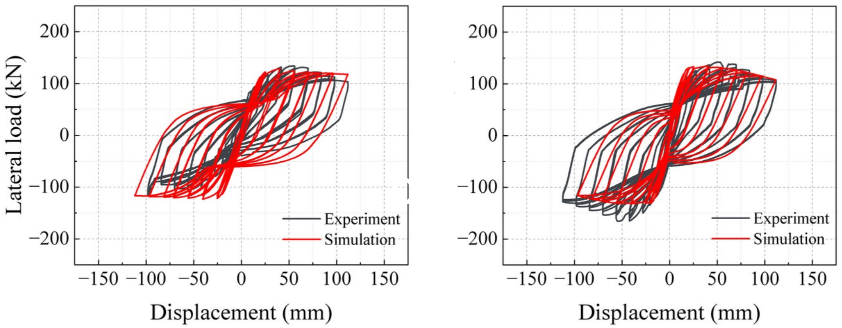

Hysteresis behaviour

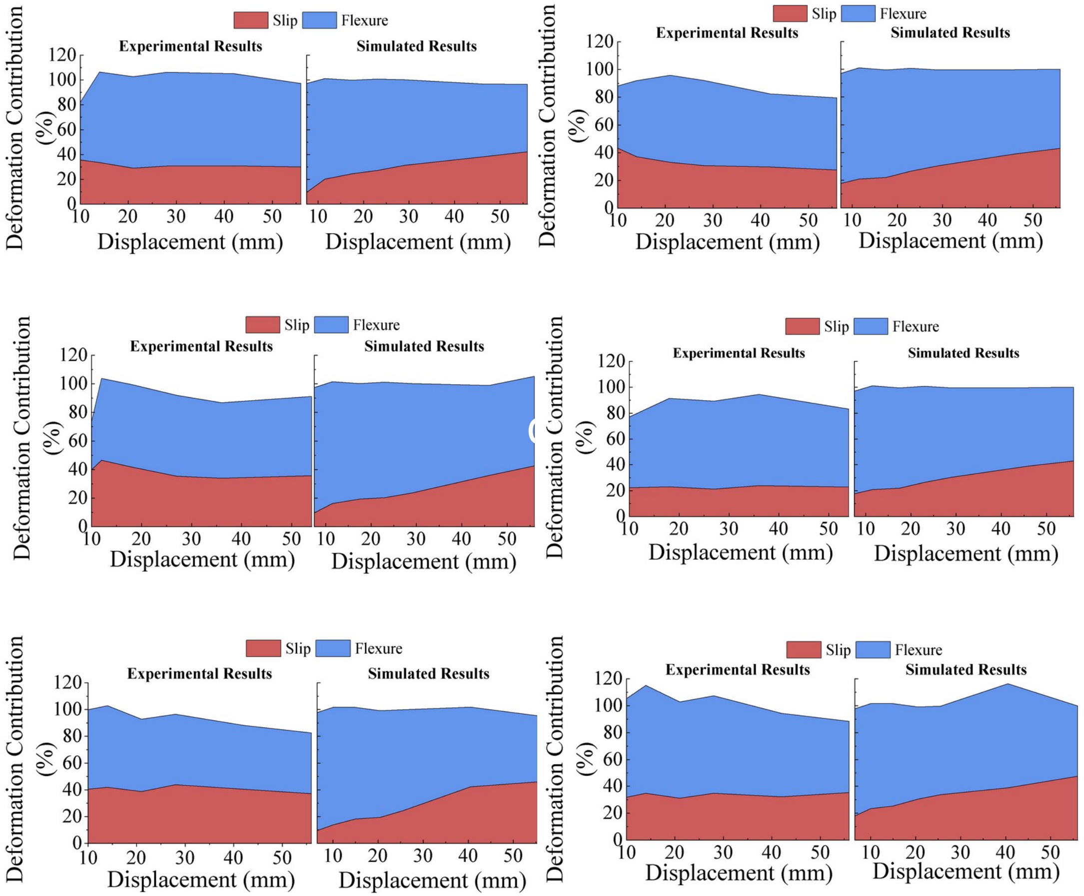

Displacement component validation

➢ The **global responses** and **displacement components** are in agreement with

Outline

1. Background
2. Quasi-static tests of SS-reinforced piers
3. Numerical Modelling of SS-reinforced piers
4. Plastic hinge model of SS-reinforced piers
5. Conclusion remarks

Plastic hinge prediction of SS-reinforced piers

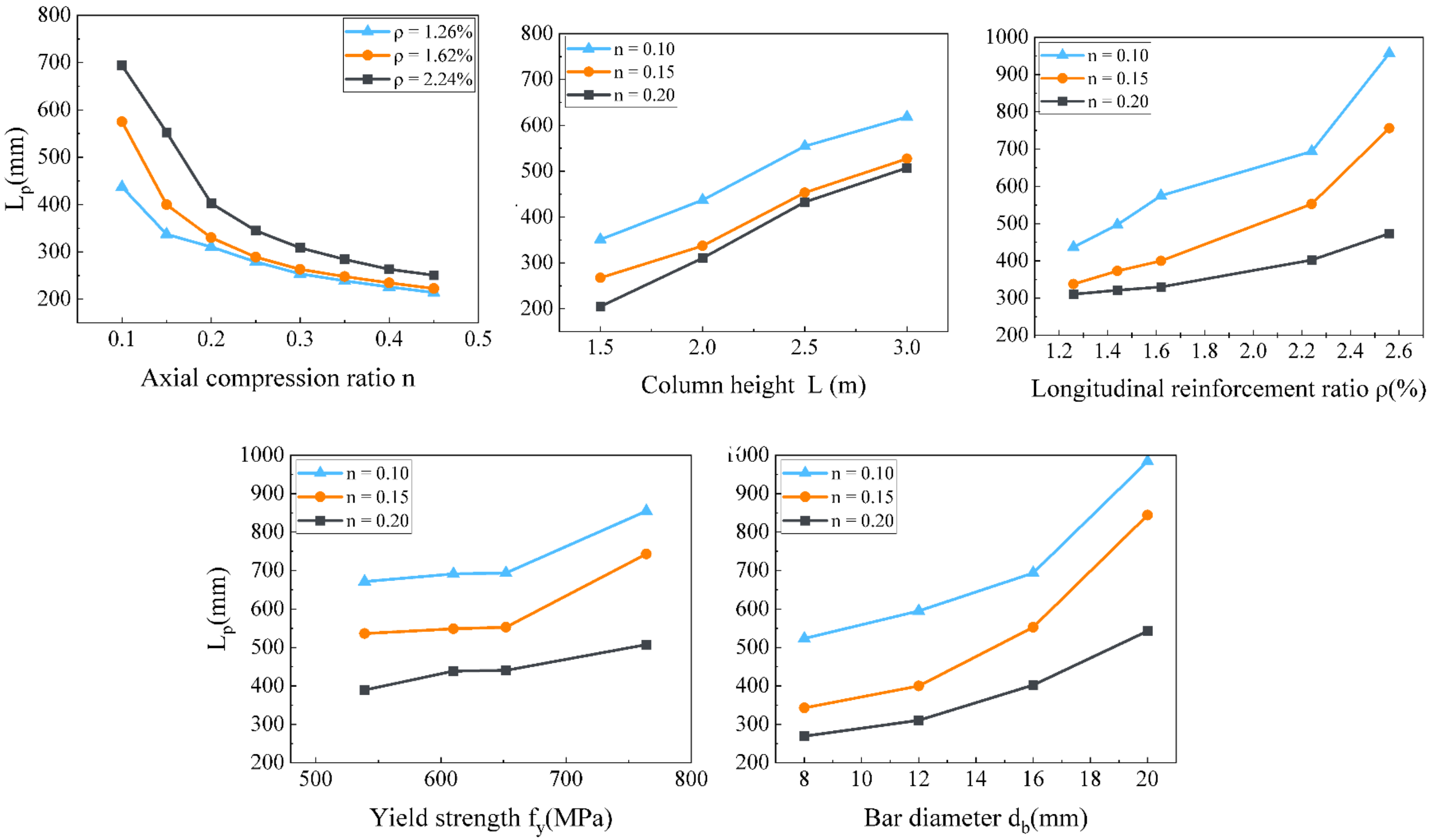

Parametric study

$$L_p = -1998.32n + 108.00\rho + 0.18403L + 0.02816(f_y d_b)$$

validation

- Axial load increases → L_p ↓
- Greater column height → L_p ↑
- Greater reinforcement ratio → L_p ↑
- Greater bar diameter → L_p ↑
- Greater yield strength → L_p ↑

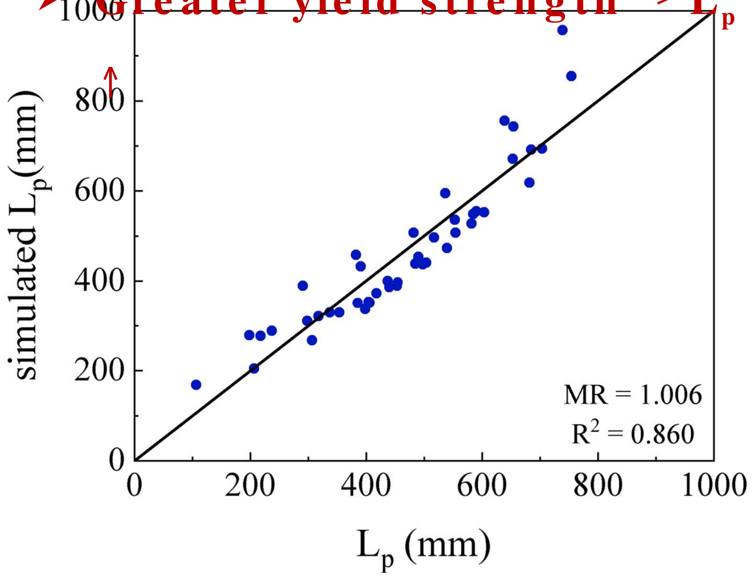

Plastic hinge prediction of SS-reinforced piers

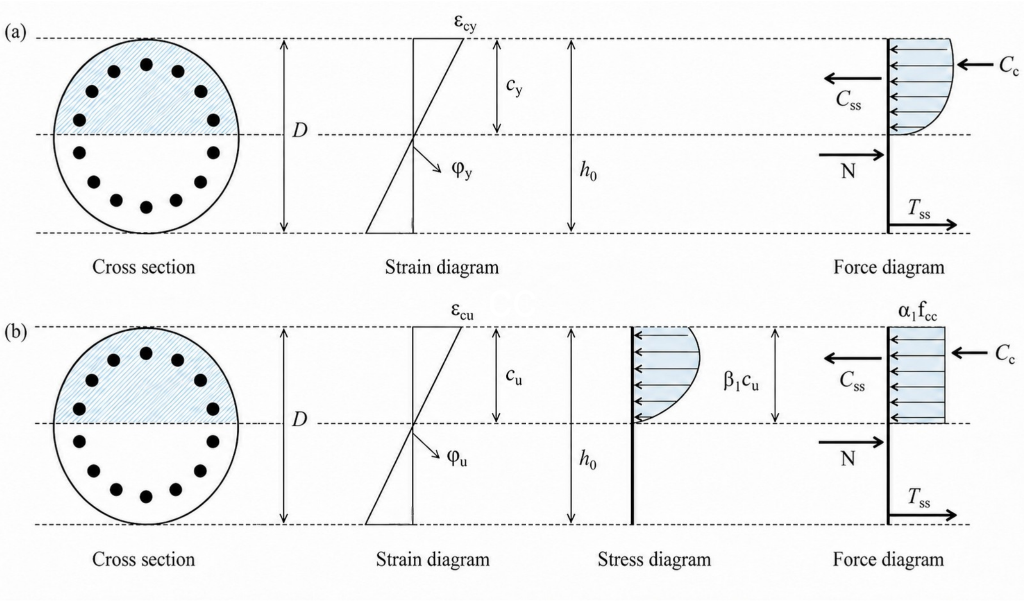

Cross-sectional strain and stress distributions

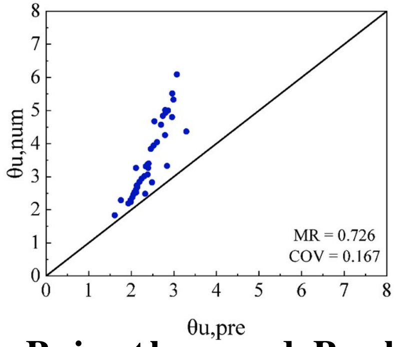

Priestley and Park (1987)

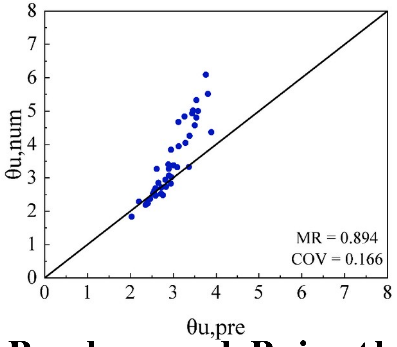

Paulay and Priestley (1992)

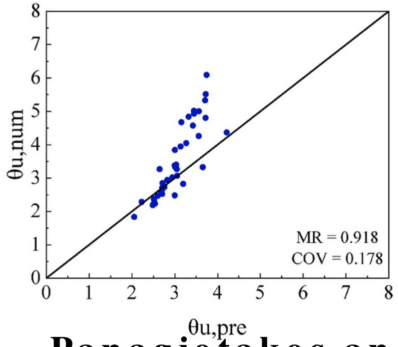

Panagiotakos and Fardis (2001)

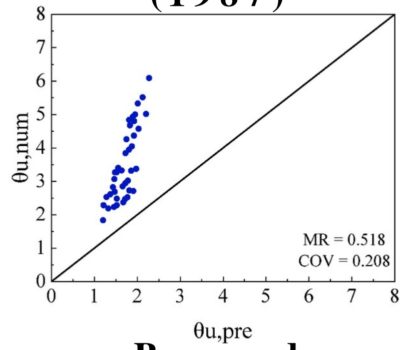

Bae and Bayrak (2008)

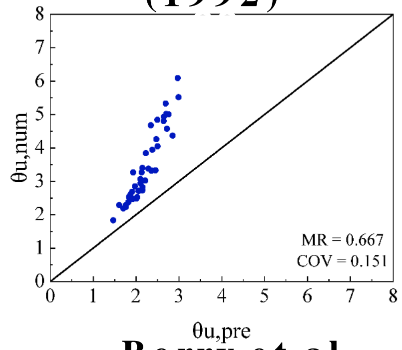

Berry et al. (2008)

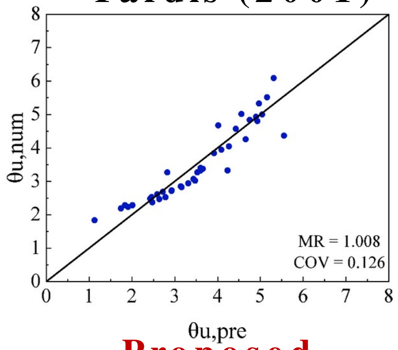

Proposed method

Comparison with other equations

- Proposed L_p equation applied to predict pier ultimate deformation & compared with existing models.
- Our predictions match numerical simulations better than other empirical formulas.

Outline

1. Background
2. Quasi-static tests of SS-reinforced piers
3. Numerical Modelling of SS-reinforced piers
4. Plastic hinge model of SS-reinforced piers
5. Conclusion remarks

5 Conclusion remark

- SS-reinforced piers exhibit **larger ultimate strength**, **deformation capacity** (drift > 5%), and **initial stiffness**, with **slower stiffness degradation** and **smaller residual displacements** than conventional CS piers.
- **Flexural deformation** dominates (70% in later stage), slip deformation remains 30–40% (reduced by higher axial load), and shear deformation is negligible (< 5%).
- The OpenSees numerical model, incorporating **inelastic buckling** and **bond-slip effects**, accurately reproduces global responses and displacement components.
- Proposed L_p equation: L_p decreases with higher axial load; increases with column height, reinforcement ratio, bar diameter, and yield strength. It predicts **ultimate deformation** better than existing models.

Thanks for your attention!